Dispersity and spinnability: Why highly polydisperse polymer solutions are desirable for electrospinning

Massachusetts Institute of Technology

Dispersity and spinnability: Why highly polydisperse polymer solutions are desirable for electrospinning

Ljiljana Palangetic,[†] Naveen Krishna Reddy,[†] Siddarth Srinivasan,[‡] Robert E. Cohen,[‡] Gareth H. McKinley,[¶] and Christian Clasen[*,†]

[†]*Department of Chemical Engineering, KU Leuven, University of Leuven, W. de Croylaan 46, B-3001 Leuven, Belgium,* [‡]*Department of Chemical Engineering, Massachusetts Institute of Technology, Cambridge, MA 02139, United States, and* [¶]*Department of Mechanical Engineering, Massachusetts Institute of Technology, Cambridge, MA 02139, United States*

E-mail: christian.clasen@cit.kuleuven.be

---

[*]To whom correspondence should be addressed
[†]Department of Chemical Engineering, KU Leuven
[‡]Department of Chemical Engineering, MIT
[¶]Department of Mechanical Engineering, MIT

Abstract

We develop new criteria that describe the minimum concentration limits controlling the spinnability of dilute and semi-dilute flexible polymer solutions with high molecular weight and varying polydispersity. By asserting that the finite and bounded extensional viscosity of the solution is the key material property determining the stability of a filament during spinning, we propose a new scaling relating the minimum necessary concentration of a polymer c_{spin} to its molecular weight M and the quality of the solvent (through the excluded volume exponent v) of the form $c_{spin} \sim M^{-(v+1)}$. This new scaling differs from the classical interpretation of the coil overlap concentration c^* or entanglement concentration c_e as the minimum concentration required to increase the viscosity of the spinning dope, and rationalizes the surprising spinnability of high molecular weight polymers at concentrations much lower than c_e. Furthermore, we introduce the concept of an extensibility average molecular weight M_L as the appropriate average for the description of polydisperse solutions undergoing an extension-dominated spinning process. In particular it is shown that this extensibility average measure, and thus the solution spinnability, is primarily determined by the extensibility of the highest molecular weight fractions. For highly polydisperse systems this leads to an effective lowering of the minimum required concentration for successful fiber spinning (in comparison to narrowly distributed polymer solutions of similar weight average molecular weights). These predictions are validated with experimental observations of the electrospinnablity of mono- and polydisperse poly(methyl methacrylate) (PMMA) solutions as well as a model bimodal blend, and through comparison to published literature data on the minimum spinnable polymer concentration for a variety of flexible long chain polymers over a range of molecular weights.

KEYWORDS:

Electrospinning· extensibility average molecular weight· narrow distribution molecular weight· polydisperse molecular weight· blends

2

Introduction

The spinning of non-woven polymeric nano- and micro-fibers has recently experienced a boost due to the discovery and re-discovery of different types of spinning techniques such as electrospinning,[1] forcespinning[2,3] and sprayspinning.[4,5] Unlike melt processing operations, these techniques yield the possibility of spinning fibers from a polymer solution at room temperature, utilizing an evaporating solvent as the means to produce a solid nano- or micro-fiber. The applications of these fibers are important both industrially and fundamentally.[1,6–14] The most widely studied technique is the electrospinning process that was originally patented in 1900 and 1902 by John Cooley[67,68] with an improved experimental setup in 1934 by Anton Formhals,[69] and popularised by Reneker's group in the 1990s.[15] During electrospinning a polymer solution acquires a surface charge as it is forced through a narrow orifice. This causes the solution to form a Taylor cone at the nozzle[16,17] from whose tip a liquid jet is ejected and accelerated towards a grounded collector. During this process the charged jet undergoes bending/whipping instabilities as a result of the inability of the jet inertia and/or tangential electromagnetic stresses to stabilize non-axisymmetric disturbances that cause the jet to stretch and its diameter to drastically reduce from millimeters to micro- or nanometers.[18] The high extension rates that this stretching induces in the jet cause the dissolved polymer chains to stretch and orient, inhibiting the breakup of the fluid jet into the corresponding electrospray that would be observed in a Newtonian fluid.[1,19] Eventually solid fibers are formed due to the high rate of solvent evaporation that results from the strongly increasing surface area of the thinning jet.[1,3]

Nearly any polymer can be spun this way as long as a solvent with the necessary volatility can be chosen, and as long as the molecular weight and the concentration are within a certain range. However, the origin of these spinnability ranges, and in particular the lower polymer concentration limit have been the subject of debate in literature.[3,5,8,10,12,26] The morphologies observed after electrospinning range from single droplets (electrospraying), to beads-on-string structures, and straight, uniform fibers. The solution parameters and properties as well as process param-

eters that control the fiber diameter and morphology are numerous and have been extensively investigated.[20–22] Parameters such as polymer concentration, molecular weight and its distribution,[23–25] solvent quality and volatility[26,28,29] (coupled with environmental conditions as solvent saturation[24,30,31]), surface tension,[32] conductivity,[33] viscosity,[34,35] viscoelasticity, flow rate, distance between the electrodes (and their configuration) as well as the applied potential difference[36] (that we indicate schematically indicate in Figure 1) form a complex set of interactions. The parameters that can be controlled can generally be divided into two groups, parameters that determine the solution properties and the experimental parameters that characterise the process. Parameters that determine the viscoelastic properties of the solution are the solvent and polymer type and concentration, as well as the polymer molecular weight and molecular weight distribution (MWD). Further solution properties include conductivity, surface tension, solvent diffusivity and mass transfer coefficients to the gas phase. These solution properties can be influenced by the environmental conditions (solvent saturation or generally gas phase composition and temperature). It is the evolution of the properties during the spinning process that determines the final fiber morphology.

The solution conductivity, in combination with the spinning geometry and the applied voltage, determines the electromechanical stress (EMS) in the fluid jet. The EMS is primarily responsible for driving the stretching deformation and the general filament thinning process. Surface pressure (and thus surface tension) is responsible for amplifying perturbations in the jet via the development of a capillary instability and thus for the formation of a beads-on-string structure. This can lead to a breakup into single droplets[35] if no other stresses develop that can resist the breakup of the thin ligament which forms between two adjacent beads. One contribution to the total stress that resists the capillary breakup process is the EMS that stretches the filament. The other resisting stress contribution that balances the local capillary thinning dynamics is the viscoelastic stress in the polymeric solution. Both, surface pressure and EMS are rather insensitive to the polymer concentration and their evolution can thus be treated approximately as being solely a function of the diameter of the stretching filament within the electric field. Initial simulations of the spinning process followed this approach and approximated the deviatoric stresses in the fluid simply as those

4

of a Newtonian liquid.[37] Several publications have associated the critical entanglement concentration c_e of the polymer being spun with the lower bound of the (constant) Newtonian viscosity necessary to sufficiently resist the capillary breakup (and thus a lower limit of the polymer concentration which we denote generally as c_{spin} required to achieve fibers).[26,34,35,38] At c_e a topological transition from an unentangled to an entangled state occurs resulting in a rapid increase in the solution viscosity.[63] However, electrospinning experiments by Yu et al.[39] and later by Helgeson et al.[43] showed subsequently that even for polymer solutions with concentrations well below c_e the capillary instability can be suppressed. They attributed the additional resisting stresses to contributions arising from the elasticity of the polymer solution. The viscoelastic stresses, and in particular their transient evolution in the straight portion of the jet, have been incorporated in simulations by selecting appropriate constitutive models, such as the upper convected Maxwell,[18] Giesekus,[40,41] the Oldroyd-B,[42] and lately a FENE-P/CDD-s model.[59]

An asymptotic simplification of these models has been discussed by Helgeson et al.[43] who assumed the dominant contribution of the viscoelastic stresses to eventually originate from the constant finite extensibility limit of the molecules, which gives rise to a large constant value of the extensional viscosity. They justified this approach by pointing out that, for a specific large value of the dimensionless stretching rate ($Wi = 10$) and a typical finite extensibility L^2, the limiting extensional viscosity η_E^∞ will be reached within the Hencky strains that the thinning jet experiences in the straight regime, i.e. before the onset of the whipping instability. They furthermore neglected subdominant contributions from inertial and surface tension stresses, which led to more physical insight into the parameters controlling the spinning process within the straight portion of the thinning jet.

What has also been neglected in the above models and asymptotic simplification is the loss of solvent that leads to an increase in concentration up to the final solidification of the fiber.[1,3,44] This simplification can be justified for the straight portion of the jet (as experimentally shown by Helgeson et al.[43]) on which these models primarily focused (and thus for radii that are still large compared to the final fiber diameter). However, it is the bending instabilities and the resulting high

local extension rates and deformations in the whipping jet that result in the pronounced viscoelastic stabilization that overcomes the increasing capillary pressure in the rapidly thinning polymeric filament. The general argument used to justify the focus on the straight portion of the jet is that at the onset of the bending instabilities the significant contribution from evaporation and the resulting increase in polymer concentration (and concomitantly in the viscoelastic stresses) is even more rapid than the increase in capillary pressure. The stabilization in the straight part of the jet is thus assumed to be convected into the bending part, so that all arguments applying to limiting bounds of the concentrations for stabilization apply also to the bending part.

In this paper we follow a similar approach and neglect the transient concentration increase during the whipping phase by a similar approximation of a 'limiting' concentration at which the spatially-evolving viscoelastic stresses are sufficient to stabilize the filament. Like Helgeson et al.[43] we approximate the physics that dominates this regime with the finite extensibility limit of the polymer chain and the associated maximum bounded extensional viscosity. With this simplification of the viscoelastic contribution to the tensile stress in the jet we are now able to perform a scaling analysis of polymer molecular weight and concentration for the minimal viscoelastic stresses (and thus the minimal necessary polymer concentration henceforth denoted c_{spin}) required to stabilize the jet sufficiently against breakup and to observe the onset of fiber formation (and we use this observable *onset* of fiber formation in all the following discussions as a criterion to classify a given polymer solution as 'spinnable' or 'electrospinnable', even though some fraction of beaded structure might still be present). This is then also experimentally accessible, since we are able to keep the other experimental variables indicated in Figure 1 constant.

In the present work, we focus on solutions of high molecular weight polymeric solutes and the viscoelastic contributions to the stress which counterbalance the capillary pressure driving the thinning process even below c_e. We address two issues in this study: 1) the role of molecular weight, and 2) the role of the molecular weight distribution on the minimum required polymer concentra-

tion for the formation of fibers. Both issues have been discussed to some extent in the literature. Initial studies indicated that the required polymer concentration for a continuous, bead-free fiber formation could be related (for a particular M_w) to the critical entanglement concentration c_e of polymer chains in solution in the semi-dilute regime (which is typically 10 times above the critical overlap concentration c^*).[63] The minimum required spinning concentration c_{spin} was in this case linked to a sufficient viscosity level in the solution.[26,34,35] For the relatively low molecular weights considered in these studies this viscosity was only achieved for high polymer concentrations $c > c_e$ where the viscoelastic stresses are dominated by coil overlap and entanglement effects.[47,48] Furthermore, since the critical overlap concentration is linked to the molecular weight of a polymer and the solvent quality, it was possible to derive a correlation between the minimum required polymer concentration and the molecular weight

$$c_{spin} \sim c^* \sim M^{(1-3\nu)} = M^{-a} \tag{1}$$

In this expression the solvent quality enters via the exponent a of the Mark-Houwink-Sakurada (MHS) equation

$$[\eta] = K_H M^a \tag{2}$$

that relates the size of an isolated coil in solution via the intrinsic viscosity $[\eta]$ to the molecular weight of the polymer chain. The exponent a is directly related to the excluded volume exponent ν of scaling theories for flexible polymer conformation in solution[51,63,64]

$$a = 3\nu - 1 \tag{3}$$

A corollary of the minimum required viscosity is a relationship between the fiber diameter and zero-shear viscosity which is found to have a power law exponent of approximately 0.8 for different polymers.[34,35]

Published studies for which these relations are observed are limited to low and moderate molec-

7

ular weight polymers ($M_w < 500$ kg/mol). For these molecular weights the chain entanglement effects at concentrations above c^* lower the magnitude of the Trouton ratio, and it is therefore less essential to focus on coil-stretch transitions resulting from the extensional character of the flow. However, as the molecular weight of the polymer increases further, the extensibility of the molecules increases and the Trouton ratio of the polymer solution can thus increase dramatically. This leads, amongst other effects, to the well documented stabilising role of small amounts of very high molecular weight species in a variety of spinning operations.[49,50,66] In order to investigate this effect of polymer extensibility and the role of extensional viscosity on the fiber formation during electrospinning, the first part of this article focuses on exploring and improving existing scalings between c_{spin} and M_w. These experiments are conducted with narrowly distributed molecular weight polymers over a broad range of molecular weights (100 kg/mol to 1700 kg/mol) and with a special focus on higher molecular weights.

The second issue addressed in this paper is the effect of polydispersity or the molecular weight distribution (MWD) of a polymer sample on the resulting morphology of the fibers and on the critical concentration regimes at which fibers are first obtained. It has been shown that fixing the concentration and increasing the polydispersity (or broadening the MWD) gives thicker fibers.[34,70] Recently, Srinivasan et al. have shown that sprayspinning a polydisperse polymer solution of the same weight average molecular weight as a monodisperse one results in more uniform, continuous fibers which they attributed to the presence of small amounts of high molecular weight species.[5] They supported this hypothesis by spinning a bimodal blend of two narrowly distributed samples of high and low molecular weight polymer with similar weight average molecular weight and concentration as the polydisperse sample. While the low molecular weight sample was non-spinnable by itself, the bimodal blend readily produced fibers with morphologies similar to that of the polydisperse sample, indicating the importance of high molecular weight species in the polymer solution. In the current study we quantify the effect of polydispersity by introducing the concept of an extensibility average molecular weight (M_L) that more accurately captures the contributions of different length chains to the total extensional stress developed in an electrospun fiber.

The text is organized as follows: in the experimental section a thorough characterization of the polymers studied in this article is carried out using static light scattering (SLS), gel permeation chromatography (GPC) and Ubbelohde viscometry in order to enable us to accurately determine different moments of the molecular weight distribution and the excluded volume exponent. In the results section we first compare the morphology of electrospun fibers using narrowly distributed polymer samples with the previously established power law scaling for $c > c_e$. We then introduce a new scaling for the high molecular weight and low concentration regime based on an estimation of the required minimum extensional stresses, and validate the predictions with experimental results obtained for dilute polymer solutions ($c < c_e$) with narrow molecular weight distribution and through comparison to published literature data on the minimum spinnable polymer concentration. Finally, the prediction of spinnability of polydisperse and bimodal samples is compared with the new scaling laws using the concept of an extensibility average molecular weight M_L that quantitatively captures the strong contributions of dilute high molecular weight species to the nanofiber spinning process.

Experimental section

Materials. To investigate fiber formation during electrospinning, different concentrations of both narrowly distributed and polydisperse poly(methyl methacrylate) (PMMA) (Polymer Source, Montreal, QC, Canada) solutions were prepared using Asahiklin AK225 (Asahi Glass Company, West Chester, PA, USA) as the solvent.[5] Asahiklin AK225 is a moderately volatile hydrochlorofluorocarbon containing 3,3-dichloro-1,1,1,2,2-pentafluoropropane (42-52 wt%) and 1,3-dichloro-1,1,2,2,3-pentafluoropropane (50-60 wt%) with a density of 1550 kg/m^3 and an interfacial tension of 16.2×10^{-3} N/m. Asahiklin AK225 has a vapour pressure of 0.385 kg/cm^2 at 25 °C and is six times more volatile than toluene.

Static light scattering (SLS). The weight average molecular weight M_w of the PMMA samples

was detected using SLS. The refractive index increment (dn/dc) was determined using an Anton Paar refractometer (Anton Paar GmbH, Graz, Austria) and a home made Michelson interferometer. For PMMA in Asahiklin AK225 we obtained dn/dc = 0.169 ml/g. An example of SLS data for different concentrations of sample N_3 (where N indicates a narrow distribution) in Asahiklin AK225 is shown in Figure 2.b. The extrapolation of the scattering data to zero concentration yielded the weight average molecular weight M_w, listed in Table 1.

Gel permeation chromatography (GPC). GPC with a refractive index detector (Breeze1525 HPLC system, Waters, Milford, MA, USA) was used to obtain the molecular weight distribution of the PMMA samples that were used to prepare solutions for electrospinning. Prior to characterization, a 5 mg/ml solution of each PMMA sample was prepared using dimethylformamide (DMF) as the solvent. The solutions were allowed to settle for $\sim$ 8 hours, and were passed through a 0.45 μm Teflon disc filter. The GPC column was initially calibrated using commercially available monodisperse PMMA standards (Polymer Source, Dorval, Canada)) in DMF. From the differential molecular weight distribution (MWD), different molecular weight moments and averages as well as the polydispersity have been calculated and are summarized in Table 1.

Ubbelohde viscometry. To obtain the parameters of the Mark-Houwink-Sakurada (MHS) equation (Eq. 2), intrinsic viscosities $[\eta]$ of PMMA samples were determined using an Ubbelohde viscometer (SCHOTT AG, Mainz, Germany). For every sample, five different concentrations of the polymer solution were prepared such that their normalized efflux time (i.e. efflux time of the polymer solution/efflux time of the pure solvent) varied between 1.5-2.2.[53] Figure 2.a shows the specific viscosity for five narrowly distributed (N_1-N_5) and one polydisperse (P_1) PMMA sample. Using the resulting intrinsic viscosities and the weight average molecular weight M_w obtained from light scattering and GPC, the MHS equation (Eq. 2) was fitted and found to be $[\eta] = 7.74 \times 10^{-6}$ $M_w^{0.754}$ (with $[\eta]$ in ml/g and M_w in g/mol), see Figure 2.d. Similar values for the MHS coefficients and exponents have been reported in literature for PMMA in other fluorocarbon solvents.[54,55]

Electrospinning. The PMMA fibers were spun using a climate controlled electrospinning

10

Table 1: Molecular weight averages, a) measured using static light scattering (SLS) for a weight average molecular weight (M_w), b) measured using gel permeation chromatography (GPC) for: the number average molecular weight (M_n), the viscosity average molecular weight (M_v, obtained from Eq. 14 using the exponent $a = 0.754$ of the the MHS equation), the weight average molecular weight (M_w), the new extensibility average molecular weight (M_L, from Eq. 18), and the polydispersity index (PDI $= M_w/M_n$) of the PMMA samples used for the electrospinning experiments.

PMMA sample	M_w(SLS) kg/mol	M_n(GPC) kg/mol	M_v(GPC) kg/mol	M_w(GPC) kg/mol	M_L (GPC) kg/mol	PDI (GPC)
N_1	106	82.5	87.5	88.0	89.2	1.06
N_2	164	125	133	134	136	1.07
N_3	330	341	367	370	376	1.08
N_4	789	665	773	783	806	1.17
N_5	1745	1376	1733	1772	1857	1.28
P_1	582	344	773	555	608	1.61

chamber EC-CLI (IME Technologies, Eindhoven, The Netherlands). The polymer solution was dispensed from a syringe with a needle of inner diameter $D_i = 0.61$ mm at a flow rate of 0.2 ml/hr using a syringe pump (Harvard Apparatus, Holliston, MA, USA). A DC voltage of 21 kV was applied between the dispensing needle and a grounded aluminum foil collector placed 18 cm apart. The spinning was performed at $22^oC \pm 0.5\ ^oC$ with 30% $\pm$3% relative humidity. The resulting electrospun fibers were imaged using a scanning electron microscope (Philips XL 30 FEG) operated at 5-10 kV.

Results and discussion

Minimum required polymer concentration

The actual required minimum concentration for electrospinning of fibers, c_{spin}, depends on the polymer/solvent system. It is determined by the balance between the EMS (that acts on the dielectric fluid and determines the extension rate $\dot{\varepsilon}$) and the viscoelastic stress in the fluid (that depends on the material properties of the polymer solution, which themselves vary with $\dot{\varepsilon}$). The apparent correlation of c_{spin} with c_e or c^* is therefore an indication that the magnitude of the fluid viscosity

is the dominant material property controlling the critical minimum fluid stress for fiber formation.

For dilute and semi-dilute polymer solutions the zero-shear viscosity is a function of c/c^* and the background solvent viscosity. This implies that for solvents of similar viscosity the critical viscosity level will be reached at similar c_{spin}/c^*. For lower molecular weight polymers McKee et al[34] and Shenoy et al[26] have shown that for the formation of uniform fibres the critical ratio c_{spin}/c^* is of the order of 10. Based on this they related the critical viscosity level to the number of interactions of the overlapping coils and observed that c_{spin} is appears to be close to the entanglement concentration c_e for which generally $c_e/c^* \sim 10$.[63] This apparent correlation has also been used by Srinivasan et al.[5] to relate c_{spin} to M_w for other forms of spraying/spinning of moderate molecular weight polymer solutions via the proportionality of c^* to the intrinsic viscosity $[\eta]$ and thus to M_w via the Mark-Hauwink-Sakurada (MHS) relation of Eq. 2.

In the present study the minimum polymer concentration necessary for fiber formation as a function of molecular weight, c_{spin}, was investigated for narrowly distributed PMMA in Asahiklin AK225. Figure 3 shows the morphology of the electrospun polymer for different molecular weights and at concentrations below and above the entanglement concentration $c_e \simeq 10c^*$ (where c^* is the coil overlap concentration evaluated from Eq. 1).

In order to compare our results to previous reports of the minimum spinning concentration we also show in Figure 3 the entanglement concentration $c_e = 10c^*$ as a function of the molecular weight. For this we evaluate c^* using the expression $c^* = 0.77/[\eta]$,[27,65] combined with our results for the Mark-Houwink-Sakurada equation (Eq. 2) for PMMA in Asahiklin of $[\eta] = 7.74 \times 10^{-6}M_w^{0.754}$ (with units of ml/mg for $[\eta]$ and g/mol for M_w) to give[51]

$$c^* = 9.95 \times 10^4 M_w^{-0.754} \tag{4}$$

Srinivasan et al.[5] also determine a relationship between c^* and M_w for PMMA in Asahiklin; however they use incorrect units in evaluating the intrinsic viscosity of PMMA in a θ-solvent. When corrected, their estimate is consistent with the expression in Eq. 4.

The SEM images given in Figure 3 for the lower molecular weight sample N_3 of 370 kg/mol

PMMA show the onset of fiber formation only when the polymer concentration is above the entanglement concentration (in this case $c_e \simeq 10c^*_{370} = 60$ mg/ml). It should be noted here that the same threshold level of fiber formation was applied for all the images in Figure 3. Similar to Shenoy et al.[26] the threshold was defined as a fraction of at least 50 % of the observable continuous fibers above a critical length; in the current case this limit was defined as fibers longer than 100 μm. For a higher molecular weight sample N_4 ($M_w = 783$ kg/mol) the fiber formation threshold is reached at a much lower concentration of 20 mg/ml, which is slightly below the entanglement concentration given by $c_e \simeq 10c^*_{783} = 30$ mg/ml. Following this trend, for sample N_5 with $M_w = 1772$ kg/mol a significant fraction of fibers are observed even at 5 mg/ml, which is already a factor of three below the respective entanglement value ($10c^*_{1772} \cong 17$ mg/ml). These results clearly show that for higher molecular weights the minimum concentration for the formation of fibers does not follow the previously assumed power law scaling of c^* (and c_e) with M_w. The actual scaling for the minimum required concentration c_{spin} observed in Figure 3, indicated by the dashed line, exhibits a much steeper slope $c_{spin} \sim M_w^{-1.5}$ than that predicted by the overlap concentration criteria of Eq. 1, $c^* \sim M_w^{-0.754}$. It should be noted that the new scaling becomes dominant at very high molecular weights. At lower molecular weight, for the same polymer/solvent system, the minimum polymer concentration for fiber formation follows the more conservative scaling previously established from overlap and entanglement concentration criteria.[5,34,35] The crossover appears to happen around a molecular weight $M_w^* = 4 \times 10^5$ g/mol.

For high molecular weights ($M > M^*$), the viscoelastic stresses that resist the general filament thinning and the development of instabilities on the jet can no longer simply be assumed to originate from the zero-shear viscosity of the spinning solution. The coil-stretch transition of the polymer chains in the strong extensional flow of the spin-line leads to a rapid increase in the viscoelastic tensile stresses. This coil-stretch transition leads eventually to a complete unravelling of the polymer chains and a saturation of the extensional viscosity in its finite extensibility limit, denoted η_E^∞. Helgeson et al.[43] argue and have experimentally verified that this limit is reached

within the straight portion of the jet before onset of any instability; the viscoelastic stresses in the later stages of the spinning process will thus be determined by the magnitude of this extensional viscosity η_E^∞. In the following we therefore seek a new scaling relation of c_{spin} to the molecular weight that incorporates the true magnitude of the viscoelastic stresses in the spin line as the chains approach their finite extensibility limit.

In dumbbell kinetic theory for dilute polymer solutions[19] the finite extensibility limit for the extensional viscosity is found to be

$$\eta_E^\infty \cong 2\eta_p L^2 \tag{5}$$

where η_p is the polymer contribution to the total shear viscosity $\eta = \eta_p + \eta_s$ (with η_s as the solvent viscosity) and L^2 is the finite extensibility of the dumbbell.[19] The polymer contribution to the total viscosity depends on the concentration and molecular weight and can be determined from the intrinsic viscosity through the expression

$$\eta_p = \eta_s[\eta]c \tag{6}$$

where the intrinsic viscosity $[\eta]$ is related to molecular weight and the excluded volume exponent via the Mark-Houwink-Sakurada equation (Eqs. 2 and 3).

The extensibility L^2 of a polymer chain and its relation to the molecular weight M of a given chain can be obtained from the mean square end to end distance $\langle R^2 \rangle$ of a single chain in a solvent at equilibrium (no flow) and in its maximum stretched length R_{max} in a strong extensional flow,

$$\langle R^2 \rangle = \alpha^2 C_\infty n l^2 \tag{7}$$

$$R_{max} = nl \sin(\theta/2) \tag{8}$$

where C_∞ is the characteristic ratio of the polymer, and n, l and θ are the bond number, length

and angle in the carbon backbone (and where $n = 2M/M_0$ for a polyvinyl chain such as PMMA, where M_0 is the molecular weight of a monomeric unit). The parameter α is the Flory expansion factor[52] in a specific solvent whose dependence on the molecular weight M and solvent quality can be described with the coil expansion coefficient k_α as

$$\alpha^2 = k_\alpha^2 \left(\frac{n \sin^2(\theta/2)}{C_\infty} \right)^{2\nu-1} \tag{9}$$

Inserting Eq. 9 into 7 yields then the known relation $\langle R^2 \rangle \sim M^{2\nu}$. From the two expressions in Eqs. 7 and 8 the finite extensibility of a flexible polymer chain in a solvent is defined as[60,61]

$$L^2 \equiv \frac{R_{max}^2}{\frac{1}{3}\langle R^2 \rangle} = AM^{2(1-\nu)} \tag{10}$$

with the constant A for a polyvinyl chain given by

$$A = \frac{3}{k_\alpha^2} \left(\frac{2 \sin^2(\theta/2)}{C_\infty M_0} \right)^{2(1-\nu)} \tag{11}$$

Substituting for L^2 and η_p from Eqs. 10 and 6 in the extensional viscosity of Eq. 5 we obtain the following expression for the limiting extensional viscosity of a dilute polymer solution

$$\eta_E^\infty \cong 2c\eta_s AK_H M^{(\nu+1)} \tag{12}$$

Assuming now a minimum required extensional viscosity $\eta_{E,spin}^\infty$ to achieve a sufficient viscoelastic stress for fiber formation during electrospinning (and also assuming that the extension rate profile at c_{spin} is independent of the molecular weight for a given polymer/solvent system), we can rewrite Eq. 12 to relate the minimum concentration required for successful fiber spinning c_{spin} and the molecular weight M of the dilute chains in the filament

$$c_{spin} \cong \frac{\eta_{E,spin}^\infty}{2\eta_s AK_H M^{(\nu+1)}} \sim M^{-(\nu+1)} \tag{13}$$

This new scaling relation can be compared to the experimental data in Figure 3, using the excluded volume exponent $\nu = 0.585$ for PMMA in Asahiklin AK225 determined from the MHS expression in Figure 2.d via Eqs. 2 and 3. We obtain $c_{spin} \sim M^{-1.585}$, which agrees well with the experimentally observed results shown in Figure 3 (dashed line).

Figure 4 also compares the new power law scaling of Eq. 13 to the minimum required polymer concentrations c_{spin} reported for other polymer/solvent mixtures in the literature, including polyvinylalcohol (PVA) in H_2O,[25] polystyrene (PS) in tetrahydrofuran (THF),[26,58] and PMMA in dimethylformamide (DMF),[35] in addition to the PMMA-AK225 studied here (Table 2 gives the various parameters of the polymer solutions and electrospinning conditions). Comparing the observed slopes in the high molecular weight regime ($M_w > M_w^*$) in Figure 4 with the respective excluded volume exponents ν in Table 2 it can be seen that previously reported literature data indeed follow the new power law scaling $c_{spin} \sim M^{(\nu+1)}$ of Eq. 13 rather than $c_{spin} \sim M^{(1-3\nu)}$ of Eq. 1 .

It should be noted again that at present Eq. 13 can only be used to predict the scaling with molecular weight, but not absolute values as we do not know the required magnitude of the viscoelastic stress for a respective polymer/solvent system. This also means that we cannot predict the specific value of the molecular weight above which the new scaling is valid. As discussed previously for lower molecular weight solutions, to quantify the required viscosity level (as characterised by $\eta_{E,spin}^{\infty}$) that is related to the stabilizing viscoelastic stress level one would need to know the evolution of the actual extension rate $\dot{\varepsilon}$ along the jet. In principle the onset of an increase in the Trouton ratio (marking the onset of visocoelastic contribution to the stabilizing stress in the filament) is governed by the Weissenberg number $Wi = \lambda\dot{\varepsilon}$ and thus numerical values for the relaxation time λ of the polymer in the specific solvent and the extension rate $\dot{\varepsilon}$ are required. The level of stress in the elongating filament and also the onset of viscoelastic stabilization thus depend on the evolution of $\dot{\varepsilon}$, which is itself dependent on the growth in the electromechanical stress (EMS) during the spinning process. The evolution of both EMS and $\dot{\varepsilon}$ are, however, spe-

cific to each polymer/solvent system and furthermore depend also on the experimental parameters indicated in Figure 1 and Table 2. This fluid specificity precludes *a priori* prediction of the transitional molecular weight and absolute values of the c_{spin} for high-molecular weight polymers. Varying the experimental conditions (such as flow rate or electric field strength) for the same polymer/solvent system will, however, affect the extension rate profile in a similar manner to varying polymer molecular weights and will thus not affect the scaling relation *per se*, but will shift the whole scaling curve (as has been reported for example by Helgeson et al.[43] who observed that changing the fluid flow rate through the spinning nozzle, for otherwise constant experimental conditions, changed spinnability).

Table 2: The experimental electrospinning parameters (applied voltage (U), separation distance between the needle and the collector (d), flow rate (Q) and the needle inner diameter (D_i)) and the polymer solution parameters (dielectric constant (ε) of the solvent and excluded volume exponent (ν)) for data reported in the literature and plotted in Figure 4.

Sample name	U (kV)	d (cm)	Q (mL/min)	D_i (mm)	ε	ν	Ref.
PMMA-AK225	21	18	0.003	0.61	4.14	0.584	
PMMA-DMF	10	15	0.05	0.7	38	0.555	[35]
PS-THF	10	35	0.07	0.51	7.6	0.566	[26,58]
PVA-H$_2$O	30	10	NA	0.16	80	0.542	[25]

Extensibility average molecular weight

Polymers used for electrospinning are typically not monodisperse but have a distribution of polymer chain lengths with molecular weights M_i for each species of length i (where i is the number of monomeric units in the chain). For simplicity, the breadth of the distribution is often expressed as a single value by the polydispersity index $PDI = M_w/M_n$ with the weight average molecular weight defined as $M_w = \sum_i N_i M_i^2 / \sum_i N_i M_i = \sum_i w_i M_i$ and the number average $M_n = \sum_i N_i M_i / \sum_i N_i = \sum_i w_i / \sum_i (w_i/M_i)$, where $w_i = c_i/c = N_i M_i / \sum_i N_i M_i$ is the weight fraction of species i and $N = \sum_i N_i$

the total number of chains. The weight average molecular weight often captures the spinning properties of a solution well, as it is close to the viscosity average

$$M_v = \left(\sum_i N_i M_i^{1+a} / \sum_i N_i M_i \right)^{1/a} = \left(\sum_i w_i M_i^a \right)^{1/a} \tag{14}$$

that gives the contribution of each species to the total zero-shear rate viscosity. However, as we have shown above, it is not the zero-shear viscosity, but rather the finite extensibility limit of the extensional viscosity that controls the spinnability of the higher molecular weight polymer solutions. In order to determine the correct moment and average molecular weight to be used for electrospinning we extend the expression for η_E^∞ given by Eq. 12 to the case of a polydisperse solution.

For a collection of polymer chains of different lengths the total polymer contribution to the extensional viscosity can be written as the sum of the contribution of each species

$$\eta_E^\infty = \sum_i \eta_{E,i}^\infty = \sum_i 2c_i \eta_s [\eta]_i L_i^2 \tag{15}$$

For each species i we can now insert the expressions for L^2 from Eq. 10, $[\eta]$ from the Mark-Houwink-Sakurada equation (Eqs. 2 and 3), as well as for the total concentration $c = \sum_i c_i = \sum_i N_i M_i / N_A$ (with N_A representing Avogadro's number) to obtain the total extensional viscosity of a polydisperse dilute solution of flexible chains at large strain rates:

$$\eta_E^\infty = \sum_i \frac{2\eta_s A K_H}{N_A} N_i M_i^{2+\nu} \tag{16}$$

Equating Eq. 16 to Eq. 12 suggests the definition of a new "extensibility average" molecular weight M_L given by

$$\eta_E^\infty = 2c\eta_s A K_H M_L^{\nu+1} \equiv \sum_i \frac{2\eta_s A K_H}{N_A} N_i M_i^{2+\nu} \tag{17}$$

and after cancelling constants which do not depend on the summation index i we obtain the fol-

lowing expression for the extensibility average molecular weight:

$$M_L = \left(\frac{\sum\limits_i N_i M_i^{2+v}}{\sum\limits_i N_i M_i} \right)^{1/(v+1)} = \left(\sum\limits_i w_i M_i^{1+v} \right)^{1/(v+1)} \tag{18}$$

Figure 5 compares the evolution of the extensibility average molecular weight M_L as a function of the polydispersity index $PDI = M_w/M_n$ for two limiting cases: a monomodal log-normal distribution function with fixed $M_w = 370$ kg/mol and secondly a bimodal blend of two narrowly distributed (log-normal) fractions of $M_{w,1} = 134$ kg/mol and $M_{w,2} = 1772$ kg/mol. The concentrations of the bimodal blend ($w_1 = 0.856$ and $w_2 = 0.144$) are selected so that the weight average molecular weight is $M_w = 370$ kg/mol, identical to the of the other solutions in Figure 5. It is clear from Fig. 5 that an increase in PDI causes a substantial increase in the extensibility average molecular weight (M_L) of a polydisperse system, which is even more pronounced for the case of the bimodal polymer solution with a small fraction of the very high molecular weight species. For the bimodal system the polydispersity index is $PDI = 2.39$ and the extensibility average molecular weight from Eq. 18 is $M_L = 579$ kg/mol even though only 14.4 wt% of the high molecular weight species is added.

To probe the rheological consequences of this extensibility average molecular weight we use the new scaling relation of Eq. 18 to re-evaluate our earlier observations. Figure 6 now also includes the morphologies obtained from electrospinning the polydisperse PMMA sample P_1, along with both the original $10c^*$-M correlation (Eq. 4) and the new c_{spin}-M (Eq. 13) power law scaling. For the polydisperse sample P_1 the fibers start to form at a concentration of $c_{spin} = 25$ mg/ml. Plotting this concentration as a function of the conventional weight average molecular weight $M_w = 555$ kg/mol of the sample would lead to an underprediction with regard to the predicted value from the new power law scaling. Only when the measured spinning concentration of the polydisperse system is plotted in terms of the (larger) extensibility average molecular weight $M_L = 608$ kg/mol (calculated from the molecular weight distribution experimentally determined in Figure 2) does

the data consistently fit with the observations from monodisperse model systems. Specifically the data points for the sample P_1 are shifted to the right so that the solution appears to consist (on average) of chains with a higher average molecular weight, leading to a nearly exact match with the predictions of the new power law scaling developed in Eq. 13.

However, it should be noted that this difference between the weight average M_w and the new extensibility average M_L evaluated for the polydisperse sample P_1 in Figure 6 results in only a small effective rescaling of the ordinate values. This is because this sample, although considered polydisperse in comparison to the monodisperse polymer standards used as references in this study, still has a polydispersity index of only 1.61, which is not high by commercial standards. To put the extensibility average molecular weight to a more rigorous test we prepared a bimodal blend that has the same extensibility average molecular weight M_L as the polydisperse sample P_1. The new mixture consists of a small amount of the monodisperse high molecular weight PMMA sample N_5 ($w_1 = 0.157$) and the low molecular weight PMMA sample N_2 ($w_2 = 0.843$). The extensibility average molecular weight $M_L = \left(w_1 M_{L,1}^{(1+\nu)} + w_2 M_{L,2}^{(1+\nu)} \right)^{1/(1+\nu)}$ = 608 kg/mol of the blend is heavily influenced by the small number of highly extensible long chains, whereas the weight average molecular weight is now only $M_w = 391$ kg/mol. Figure 7 shows the morphology of the electrospun fibers of the bimodal blend at three selected concentrations (diluted from a master batch with an overall concentration of $c = 55.2$ mg/ml). When plotted as a function of the weight average molecular weight M_w the critical concentrations c_{spin} at which fibers are first produced in the electrospinning process fall far below the prediction of the new power law scaling and below the original scaling also. Plotting the same data in terms of M_L (i.e. the extensibility average molecular weight of the blend) matches the new power law scaling nearly exactly. The effects of the low weight fraction of the long chains in the blend are amplified by the very large ratio of the chain extensibilities and the resulting large contributions to the total extensional viscosity of the spinning solution. This more rigorous spinnability test suggests that the extensibility average molecular weight (M_L) is the correct moment of a polydisperse system for constructing and under-

standing the morphology and operating state diagram for electrospinning.

CONCLUSIONS

A new state diagram and concentration-molecular weight scaling has been constructed for electrospinning solutions of narrow distribution, polydisperse and blended polymer samples. For polymer samples with low molecular weights, the necessary condition for fiber formation follows the scaling law obtained from coil overlap and entanglement considerations $c_e \simeq 10c^* \sim M^{(1-3\nu)}$. For high molecular weight polymer samples we suggest a new power law scaling $c_{spin} \sim M^{-(\nu+1)}$. The new power law scaling is based on the assumption that the minimum required viscoelastic stress for fiber formation is proportional to the steady state extensional viscosity of the flexible polymer solution at high strain rates and thus to the finite extensibility of the polymer chains.

For dilute concentrations of high molecular weight polymers it is thus clear that the electrospinning process is controlled by the finite extensibility limit of the extensional viscosity η_E^∞ of the solution. We have shown that for polydisperse polymer solutions the correct measure of the average molecular weight to be used in this new power law scaling is not the conventional weight average M_w or second moment, but an extensibility average molecular weight, $M_L = \left(\sum_i w_i M_i^{(1+\nu)} \right)^{1/(1+\nu)}$. For a narrow molecular weight distribution polymer where $M_w \cong M_L$, the selection of a "correct" molecular weight average is only of minor importance. However, we have shown in Figure 7 that, for bimodal blends or samples with a broad distribution of molecular weights (and thus large values of the *PDI*), the choice of the correct moment of the chain length distribution is crucial for understanding and predicting the minimum required concentration c_{spin} for fiber formation. Figure 8 shows the new operating state diagram with the two power law scalings that are appropriate for low and high molecular weights. The concept of an extensibility average molecular weight (denoted M_L) that more appropriately reflects the contributions of even a small fraction of

21

very long and extensible chains may also help rationalise our understanding of other extensional dominated processes such as the spinning of silk[62] or commercial polyolefins of different grades (which may contain very small fractions of high molecular weight species) as well as a wide range of electrospinning, sprayspinning and force spinning processes used for the creation of non-woven nano-fiber mats.

Acknowledgement

References

1. Reneker, D.H.; Yarin A.L.; Zussman, E.; Xu, H. Electrospinning of Nanofibers from Polymer Solutions and Melts. *Advances in applied mechanics* **2007**, *41*, 43-195.

2. Lozano, K.; Sarkar, K. Methods and apparatuses for making superfine fibers. *US20090280325 A1*.

3. Mellado, P.; McIlwee, H.A.; Badrossamay, M.R.; Goss, J.A. Mahadevan, L.; Parker, K.K. A simple model for nanofiber formation by rotary jet-spinning. *Applied Physics Letters* **2011**, *99*, 203107-1-3.

4. Medeiros, E.S.; Glenn, G. M,; Klamczynski, A.P.; Orts, W.J.; Mattoso, L. H. C. Solution

Blow Spinning: A New Method to Produce Micro- and Nanofibers from Polymer Solutions. *Journal of Applied Polymer Science* **2009**, *113*, 2322-2230.

5. Srinivasan, S.; Chhatre, S.S.; Mabry, J.M.; Cohen, R.E.; McKinley, G.H. Solution spraying of poly(methyl methacrylate) blends to fabricate microtextured, superoleophobic surfaces. *Polymer* **2011**, *52*, 3209-3218.

6. Whitesides, G. M.; Mathias, J. P.; Seto, C. T. Molecular self-assembly and nanochemistry - a chemical strategy for the synthesis of nanostructures. *Science* **1991**, *254*, 1312-1319.

7. Li W. J.; Laurencin C. T.; Caterson E. J.; Tuan R. S.; Ko F. K. Electrospun nanofibrous structure: a novel scaffold for tissue engineering. *J. Biomed. Mater. Res.* **2002**, *60*, 613-621.

8. Huanga Z.-M,; Zhangb, Y.-Z.; Kotakic, M.; Ramakrishna S. A review on polymer nanofibers by electrospinning and their applications in nanocomposites. *Composites Science and Technology* **2003**, *63*, 2223-2253.

9. Xua, C.Y.; Inaic, R.; Kotakib, M.; Ramakrishna S. Aligned biodegradable nanofibrous structure: a potential scaffold for blood vessel engineering. *Biomaterials* **2004**, *25*, 877-886.

10. Ramakrishna, S.; Fujihara, K.; Teo, W. -E.; Yong, T.; Ma, Z.; Ramaseshan, R. Electrospun nanofibers: solving global issues. *Materials Today* **2006**, *9*, 40-50.

11. Bellan, L. M; Cross, J. D.; Strychalski, E. A.; Moran-Mirabal, J.; Craighead H. G. Individually Resolved DNA Molecules Stretched and Embedded in Electrospun Polymer Nanofibers. *Nano Letters* **2006**, *6*, 2526-2530.

12. Pham, Q. P.; Sharma, U.; Mikos, A. G. Electrospinning of Polymeric Nanofibers for Tissue Engineering Applications: A Review. *Tissue Eng.* **2006**, *12*, 1197-1211.

13. Tuteja, A.; Choi, W.; Ma, M.; Mabry, J.M.; Mazzella, S.A.; Rutledge, G.C.; Cohen, R.E.; McKinley, G.H. Designing Superoleophobic Surfaces. *Science* **2007**, *318*, 1618-1622.

14. Tuteja, A.; Choi, W.; McKinley, G.H.; Cohen, R.E.; Rubner, M.F. Design Parameters for Superhydrophobicity and Superoleophobicity, *MRS Bulletin* **2008**, *33*, 752-758.

15. Doshi, J.; Reneker, D.H. Electrospinning process and applications of electrospun fibers. *Journal of Electrostatics* **1995**, *35*, 151-160.

16. Taylor, G. I. Disintegration of Water Droplets in an Electric Field. *Proc. R. Soc. Lond. A* **1964**, *280*, 383-397.

17. Yarin, A. L.; Koombhongse, S.; Reneker D. H. Taylor cone and jetting from liquid droplets in electrospinning of nanofibers. *J. Appl. Phys.* **2001**, *90*, 4836-4846.

18. Yarin, A. L.; Koombhongse, S.; Reneker, D. H. Bending instability in electrospinning of nanofibers. *J. Appl. Phys.* **2001**, *89*, 3018-3026.

19. Clasen, C.; Plog, J. P.; Kulicke, W. M.; Owens, M.; Macosko, C.; Scriven, L. E.; Verani, M.; McKinley G. H.; How dilute are dilute solutions in extensional flows? *Journal of Rheology* **2006**, *50*, 849-881.

20. Deitzel, J. M.; Kleinmeyer, J. D.; Hirvonen, J. K.; Tan, N. C. B. Controlled deposition of electrospun poly(ethylene oxide) fibers. *Polymer* **2001**, *42*, 8163-8170.

21. Agarwal, S.; Wendorff, J. H.; Greiner, A. Use of electrospinning technique for biomedical applications. *Polymer* **2008**, *26*, 5603-5621.

22. Beachley, V; Wen, X. Effect of electrospinning parameters on the nanofiber diameter and length. *Materials Science and Engineering: C* **2009**, *30*, 663-668.

23. Tirtaatmadja, V.; McKinley, G. H.; Cooper-White, J. J.; Drop formation and breakup of low viscosity elastic fluids: Effects of molecular weight and concentration. *Phys. Fluids* **2006**, *18*, 043101-1-18.

24. Casper, C. L.; Stephens, J. S.; Tassi, N. G.; Chase, D. B.; Rabolt, J. F. Controlling Surface Morphology of Electrospun Polystyrene Fibers: Effect of Humidity and Molecular Weight in the Electrospinning Process. *Macromolecules* **2004**, *37*, 573-578.

25. Jun, Z.; Hou, H.; Wendorff, J. H.; Greiner A. Poly(vinyl alcohol) nanofibres by electrospinning: influence of molecular weight on fibre shape. *e-Polymers* **2005**, *38*, 1-7.

26. Shenoy, S. L.; Batesa, W. D.; Frischb, H. L.; Wnek G.E. Role of chain entanglements on fiber formation during electrospinning of polymer solutions: good solvent, non-specific polymer-polymer interaction limit. *Polymer* **2005**, *9*, 3372-3384.

27. Graessley W.W. Polymer-chain dimensions and the dependence of viscoelastic properties on concentration, molecular-weight and solvent power. *Polymer* **1980**, *21*, 258-262.

28. Guenthner, A. J.; Khombhongse, S.; Liu, W.; Dayal, P.; Reneker, D. H; Kyu T. Dynamics of Hollow Nanofiber Formation During Solidification Subjected to Solvent Evaporation. *Macromol. Theory Simul.* **2006,**, *15*, 87-93.

29. Tripatanasuwan, S.; Zhong, Z.; Reneker D. H. Effect of evaporation and solidification of the charged jet in electrospinning of poly(ethylene oxide) aqueous solution. *Polymer* **2007**, *48*, 5742-5746.

30. Therona, S. A.; Zussman, E.; Yarin, A. L. Experimental investigation of the governing parameters in the electrospinning of polymer solutions. *Polymer* **2004**, *45*, 2017-2030.

31. Deitzel, J. M.; Kleinmeyer, J.; Harris, D.; Tan, N.C.B. The effect of processing variables on the morphology of electrospun nanofibers and textiles. *Polymer* **2001**, *42*, 261-272.

32. Regev, O.; Vandebril, S.; Zussman, E.; Clasen, C. The role of interfacial viscoelasticity in the stabilization of an electrospun jet. *Polymer* **2010**, *56*, 2611-2620.

33. Bhattacharjee, P. K.; Schneider, T. M.; Brenner, M. P.; McKinley, G. H.; Rutledge G. C. On the measured current in electrospinning. *J. Appl. Phys.* **2010**, *107*, 044306-1-7.

34. McKee, M .G.; Wilkes, G. L.; Colby, R. H.; Long, T. M. Correlations of Solution Rheology with Electrospun Fiber Formation of Linear and Branched Polyesters. *Macromolecules* **2004**, *37*, 1760-1767.

35. Gupta, P.; Elkins, C.; Long T.E.; Wilkes, G.L. Electrospinning of linear homopolymers of poly(methyl methacrylate): exploring relationships between fiber formation, viscosity, molecular weight and concentration in a good solvent. *Polymer* **2005**, *46*, 4799-4810.

36. Tan, S. H.; Inai, R.; Kotaki, M; Ramakrishna, S. Systematic parameter study for ultra-fine fiber fabrication via electrospinning process. *Polymer* **2005**, *46*, 6128-34.

37. Hohman, M. M.; Shin, M.; Rutledge, G. C.; Brenner, M. P. Electrospinning and electrically forced jets. I. Stability theory. *Phys. Fluids* **2001**, *13*, 2201-2220.

38. McKee, M. G.; Layman, J. M.; Cashion M. P.; Long, T. E. Phospholipid Nonwoven Electrospun Membranes, *Science* **2006**, *311*, 353-355.

39. Yu, J. H.; Fridrikh, S. V.; Rutledge, G. C. The Role of Elasticity in the Formation of Electrospun Fibers. *Polymer* **2006**, *47*, 4789-4797.

40. Feng J. J. The stretching of an electrified non-Newtonian jet: A model for electrospinning. *Phys. Fluids* **2002**, *14*, 3912-3926.

41. Feng J. J. Stretching of a straight electrically charged viscoelastic jet *Journal of Non-Newtonian Fluid Mechanics* **2003**, *116*, 55-70.

42. Carroll, C. P.; Joo, Y. L. Electrospinning of viscoelastic Boger fluids: Modeling and experiments. *Phys. Fluids* **2006**, *18*, 053102-1-14.

43. Helgeson, M. E.; Grammatikos, K. N.; Deitzel, J. M.; Wagner, N. J. Theory and kinematic measurements of the mechanics of stable electrospun polymer jets. *Polymer* **2008**, *49*, 2924-2936.

44. Luo, C.J.; Nangrejo, M.; Edirisinghe, M. A novel method of selecting solvents for polymer electrospinning. *Polymer* **2010**, *51*, 1654-1662.

45. Fashandi, H.; Karimi, M. Pore formation in polystyrene fiber by superimposing temperature and relative humidity of electrospinning atmosphere. *Polymer* **2012**, *53*, 5832-5849.

46. Anna, S. L.; McKinley, G. H.; Nguyen, D. A.; Sridhar, T.; Muller, S. J.; Huang, J.; James, D. F. An Inter-Laboratory Comparison of Measurements from Filament-Stretching Rheometers Using Common Test Fluids. *J. Rheol.* **2001**, *45*, 83-114.

47. Clasen, C. Capillary Breakup Extensional Rheometry of Semi-dilute Polymer Solutions. *Korea-Australia Rheology Journal* **2010**, *22*, 331-338.

48. Clasen, C.; Phillips, P. M.; Palangetic, L.; Vermant J. Dispensing of Rheologically Complex Fluids: the Map of Misery. *AIChE Journal* **2012**, *56*, 3242-3255.

49. Wittmer, C. R.; Hu, X.; Gauthier, P.-C.; Weisman, S.; Kaplan, D.L., Sutherland T. D. Production, structure and in vitro degradation of electrospun honeybee silk nanofibers. *Acta Biomaterialia* **2011**, *7*, 3789-3795.

50. Wittmer, C. R.; Claudepierre, T.; Reber, M.; Wiedemann, P.; Garlick, J. A.; Kaplan, D.; Egles, C. Multifunctionalized Electrospun Silk Fibers Promote Axon Regeneration in the Central Nervous System. *Adv. Funct. Mater.* **2011**, *21*, 4232-4242.

51. Rubinstein, M.; Colby, R.H. *Polymer Physics*; Oxford University Press Inc., New York, 2003.

52. Flory, P. J. *Principles of Polymer Chemistry*; Cornell University Press Inc., Ithaca, 1953.

53. Kulicke, W-M,; Clasen, C. *Viscosimetry of Polymers and Polyelectrolytes*; Springer-Verlag, Berlin, Heidelberg, 2004.

54. Hamori, E.; Prusinowski, L.R.; Sparks, P.G.; Hughes R. E. Intrinsic Viscosity Studies of Stereoregular Poly(methyl methacrylate) in 2,2,3,3-Tetrafluoropropanol. *J. Phys. Chem.* **1965**, *69*, 1101-1105.

55. Lathova, E.; Lath, D.; Pavlinec J. The behaviour of poly(2-ethylhexyl acrylate) in dilute solution: viscosity measurements. *Polymer Bulletin* **1993**, *30*, 713-718.

56. Dell'erba R. Measurement of the Mark-Houwink constant of ultra high molecular mass poly(methylmethacrylate) in toluene. *J. Material Science Letters* **2001**, *20*, 371-373.

57. Chen, Y.-J.; Li, J.; Hadjichristidis, N.; Mays J.W. Mark-Houwink-Sakurada coefficients for conventional poly(methyl methacrylate) in tetrahydrofuran. *Polymer Bulletin* **1993**, *30*, 575-578.

58. Megelski, S.; Stephens, J.S.; Chase, D.B.; Rabolt, J.F. Micro- and Nanostructured Surface Morphology on Electrospun Polymer Fibers. *Macromolecules* **2002**, *35*, 8456-8466.

59. Prabhakar, R., personal communication.

60. Szabo, P.; McKinley, G.H.; Clasen C. Constant force extensional rheometry of polymer solutions. *Journal of Non-Newtonian Fluid Mechanics* **2012**, *169-170*, 26-41.

61. Campo-Deano, L.; Clasen C. The slow retraction method (SRM) for the determination of ultra-short relaxation times in capillary breakup extensional rheometry experiments. *Journal of Non-Newtonian Fluid Mechanics* **2010**, *165*, 1688-1699.

62. Jin, H.J.; Fridrikh, S.V.; Rutledge, G.H.; Kaplan, D.L. Electrospinning Bombyx mori silk with poly(ethylene oxide). *Biomacromolecules* **2002**, *3*, 1233-1239.

63. Colby, R.H. Structure and linear viscoelasticity of flexible polymer solutions: comparison of polyelectrolyte and neutral polymer solutions. *Rheologica Acta* **2010**, *49*, 425-442.

64. de Gennes, P.G. *Scaling Concepts in Polymer Physics*; Cornell University Press, Ithaca, 1979.

65. Graessley, W.W. *Polymer Liquids and Networks: Structure and Properties*; Garlan Science, London, 2004.

66. Saquing, C.D.; Tang, C.; Monian, B.; Bonino, C.A.; Manasco, J.L.; Alsber, E.; Khan, S.A. Alginate-Polyethylene Oxide Blend Nanofibers and the Role of the Carrier Polymer in Electrospinning *Ind. Eng. Chem. Res.* **2013**, *52*, 8692-8704.

67. Cooley, J.F. Improved Methods of and Apparatus for Electrically Separating the Relatively Volatile Liquid Component from the Component of the Relatively Fixed Substances of Composite Fluids. **1900**, UK Patent 6385.

68. Cooley, J.F. Apparatus for electrically Dispersing Fluids. **1902**, US Patent 692631.

69. Formhals, A. Process and Apparatus For Preparing Artificial Threads. **1934**, US Patent 1975504.

70. Zeng, J.; Hou, H.; Wendorff, J.H.; Greiner, A. Poly(vinyl alcohol) nanofibres by electrospinning: influence of molecular weight on fibre shape. *e-Polymers* **2005**, *5*, 387-393.
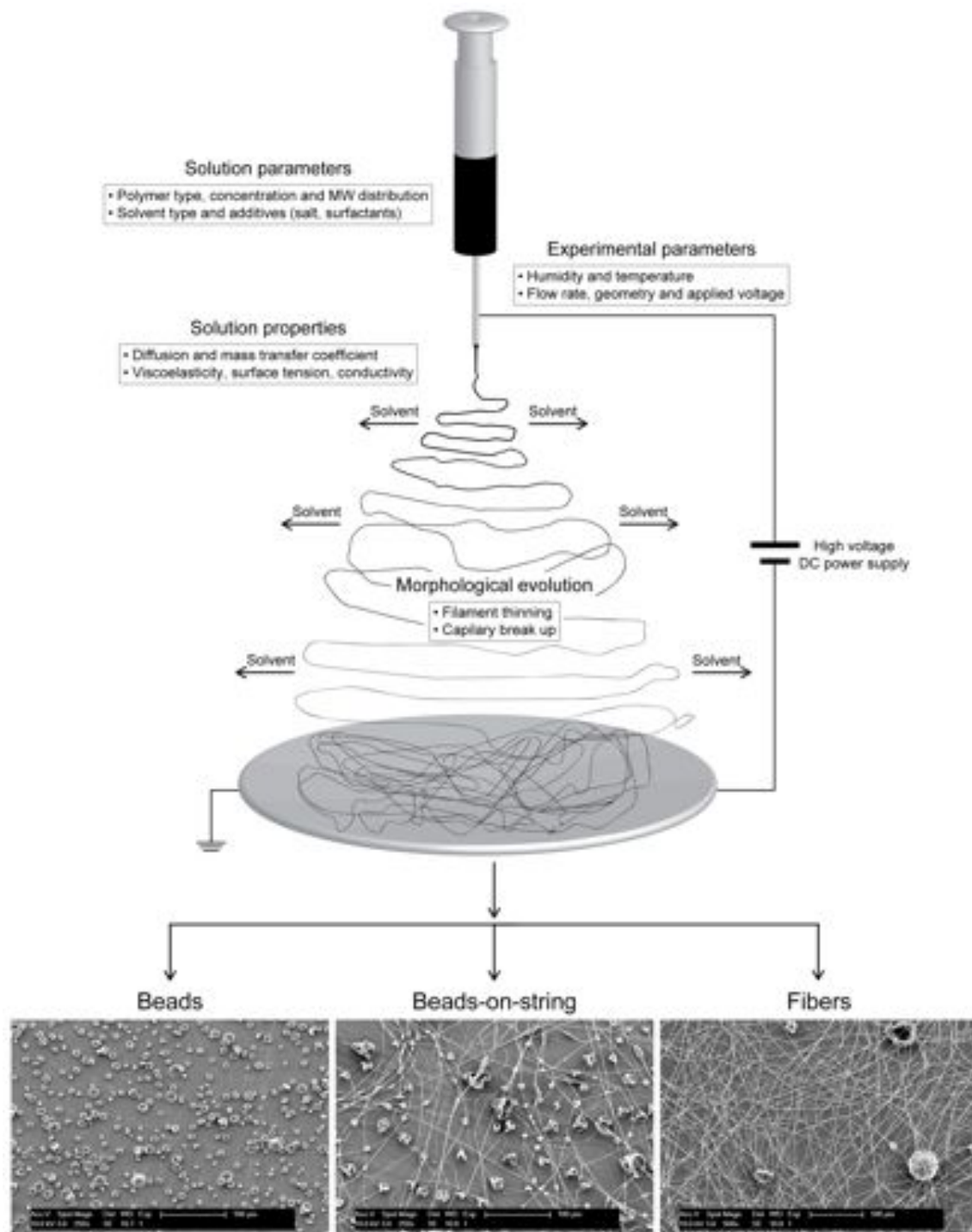
Figure 1: Schematic showing the final morphologies such as beads, beads-on-string and fibers that depend on complex interactions among different thinning and breakup processes and the experimental parameters that control the varying properties of the electrified fluid jet during electrospinning.
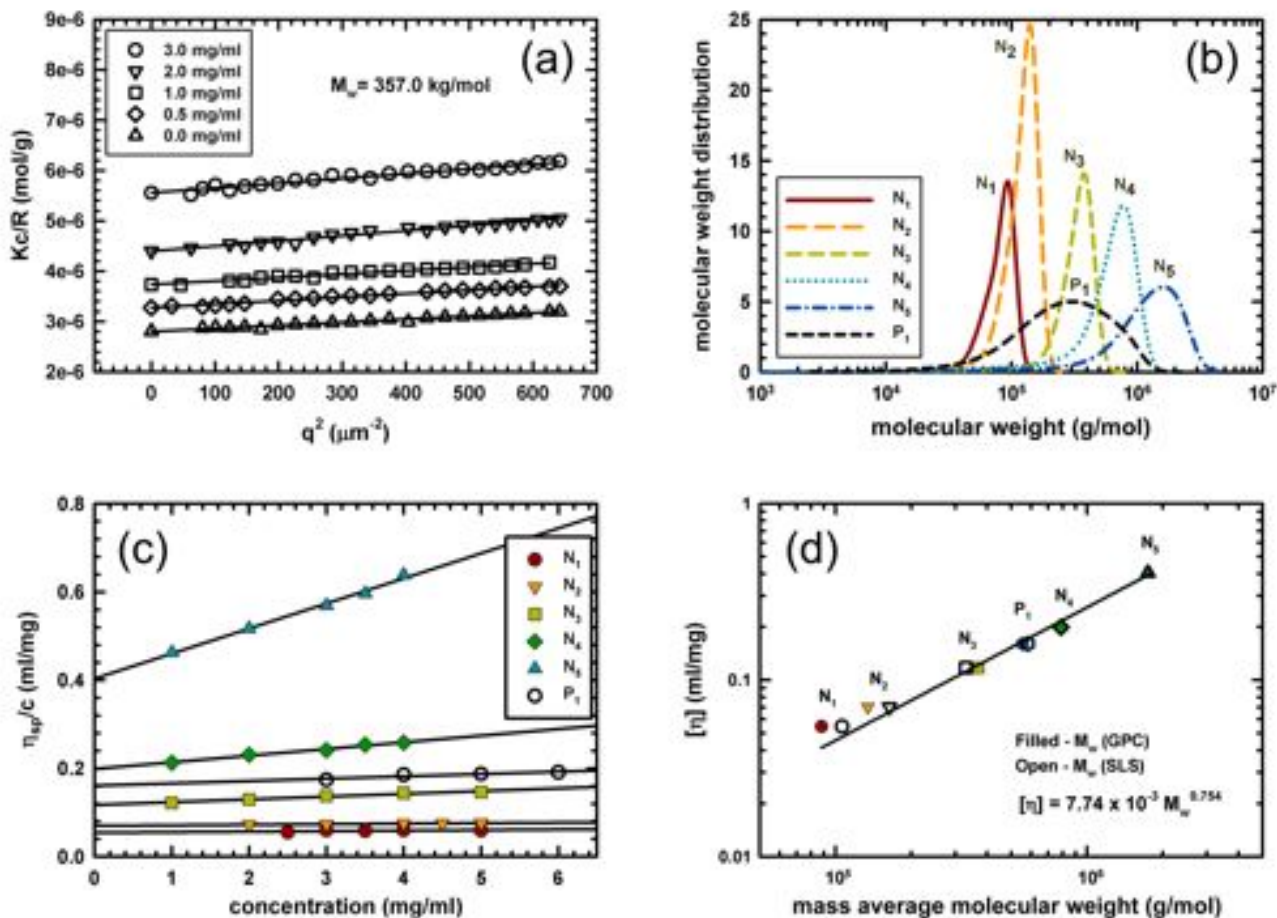
Figure 2: Characterization of five narrowly distributed (N_1 - N_5) and one polydisperse PMMA sample (P_1). a) Ubbelohde viscometry (Asahiklin AK225 as the solvent), reduced viscosity as a function of the concentration with the y-axis intercept of the linear fit giving the intrinsic viscosity [η]. b) An example of SLS data (Asahiklin AK225 as the solvent) for a narrowly distributed PMMA sample (N_3) at different concentrations as a function of the squared scattering vector (q^2). c) Gel permeation chromatography (GPC) with dimethylformamide as the solvent for different PMMA samples. The molecular weight moments calculated from these data are listed in Table 1. d) Plot of the intrinsic viscosity as a function of weight average molecular weight (open symbols are from SLS and filled symbols are from GPC). A power law fit to the data gives the Mark-Houwink-Sakurada relation (Eq. 2).
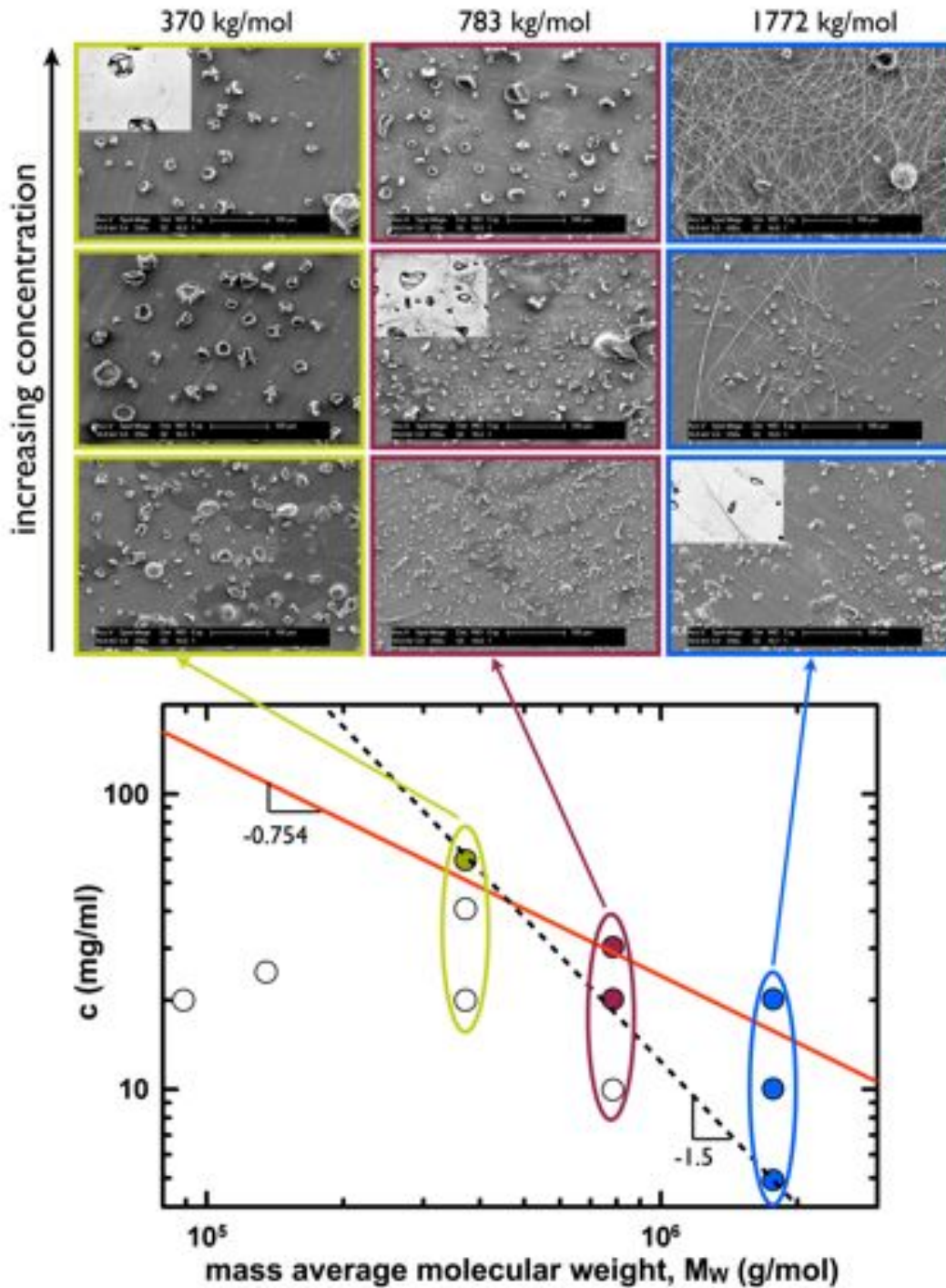
Figure 3: A plot of concentrations of PMMA in Asahiklin AK225 at which electrospinning was performed as a function of M_w. The solid line represents the traditional concentration limit ($c_e = 10c^* = 9.95 \times 10^5 \, M_w^{-0.754}$) obtained from Eq. 4. The open circles represent concentrations for which no fibers were produced, and filled circles concentrations where fibers were formed. The dashed line connects the lowest PMMA concentrations for different M_w at which the fibers were formed via electrospinning. The slope of the new dashed line is $c \sim M_w^{-1.5 \pm 0.08}$. The inserts in the images showing the onset of fiber formation are 100 μm wide.
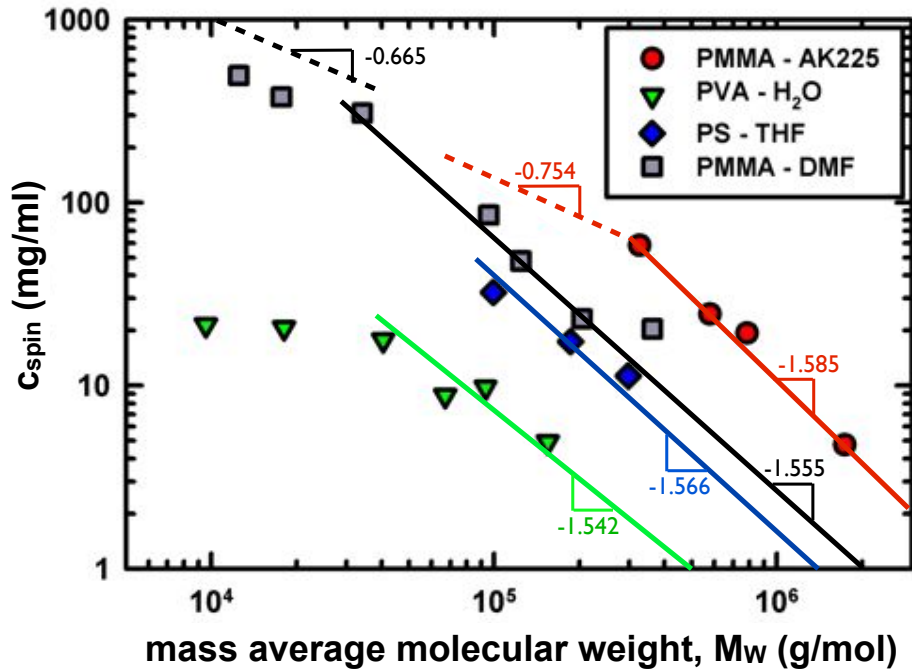
Figure 4: Lowest concentrations c_{spin} required for fiber formation of different polymer/solvent mixtures as a function of M_w taken from literature[25,26,35,58] along with c_{spin} for PMMA in Asahiklin (AK225) taken from Figure 3. The solid lines represent best fits of the new relation obtained for dilute solutions of high molecular weight given by Eq. 13. Dashed lines are critical concentrations given by $c_e = 10c^*$ of the PMMA in DMF and Asahiklin respectively which scale as $M_w^{(1-3v)}$.
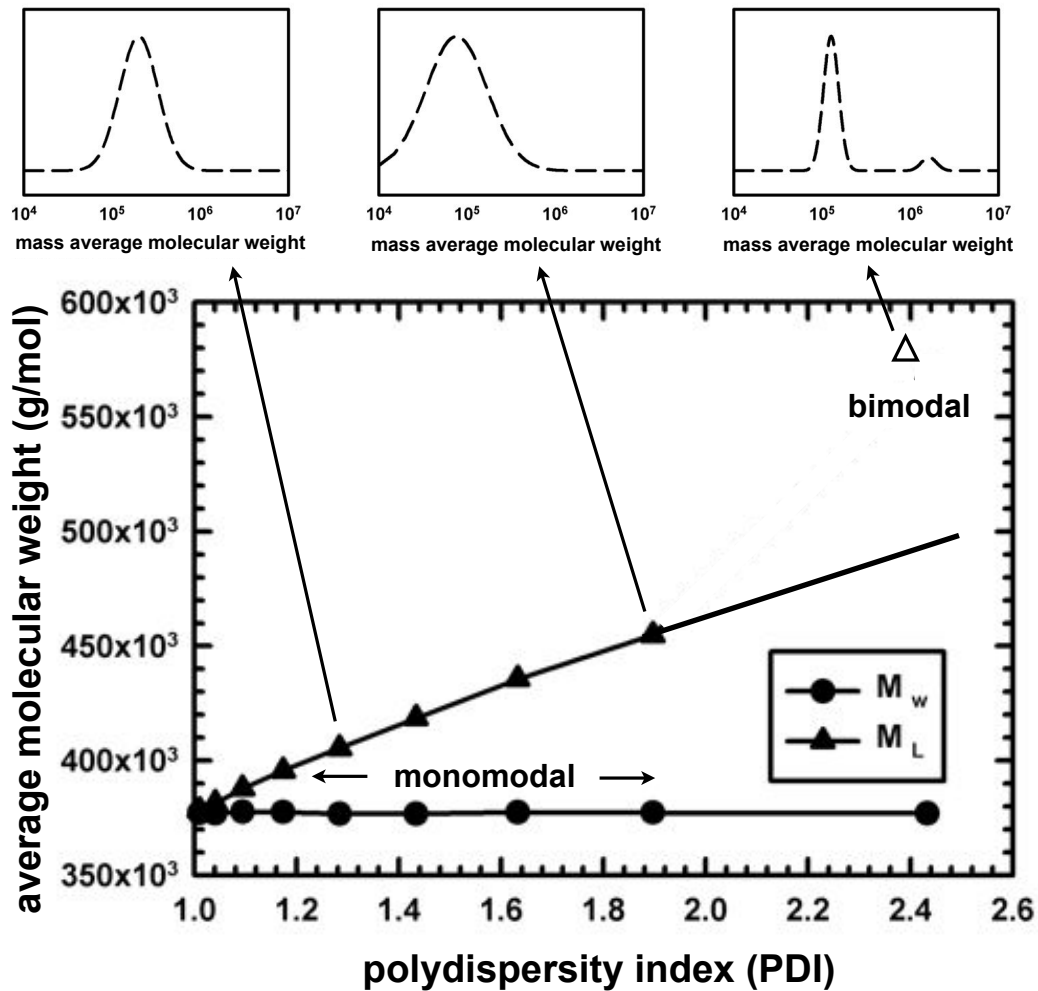
Figure 5: Evolution of the extensibility average molecular weight (M_L, triangular symbols, calculated from Eq. 18) for a given weight average molecular weight (M_w = 370 kg/mol, circular symbols, chosen to be the same as of the narrowly distributed polymer solution, N_3) as a function of polydispersity index (PDI). The simulated molecular weight distributions correspond to a monomodal log-normal distribution (closed symbols), except for the last data point (open symbol) which is for a bimodal blend of two narrowly distributed log-normal molecular weight distributions as indicated in the diagram above.
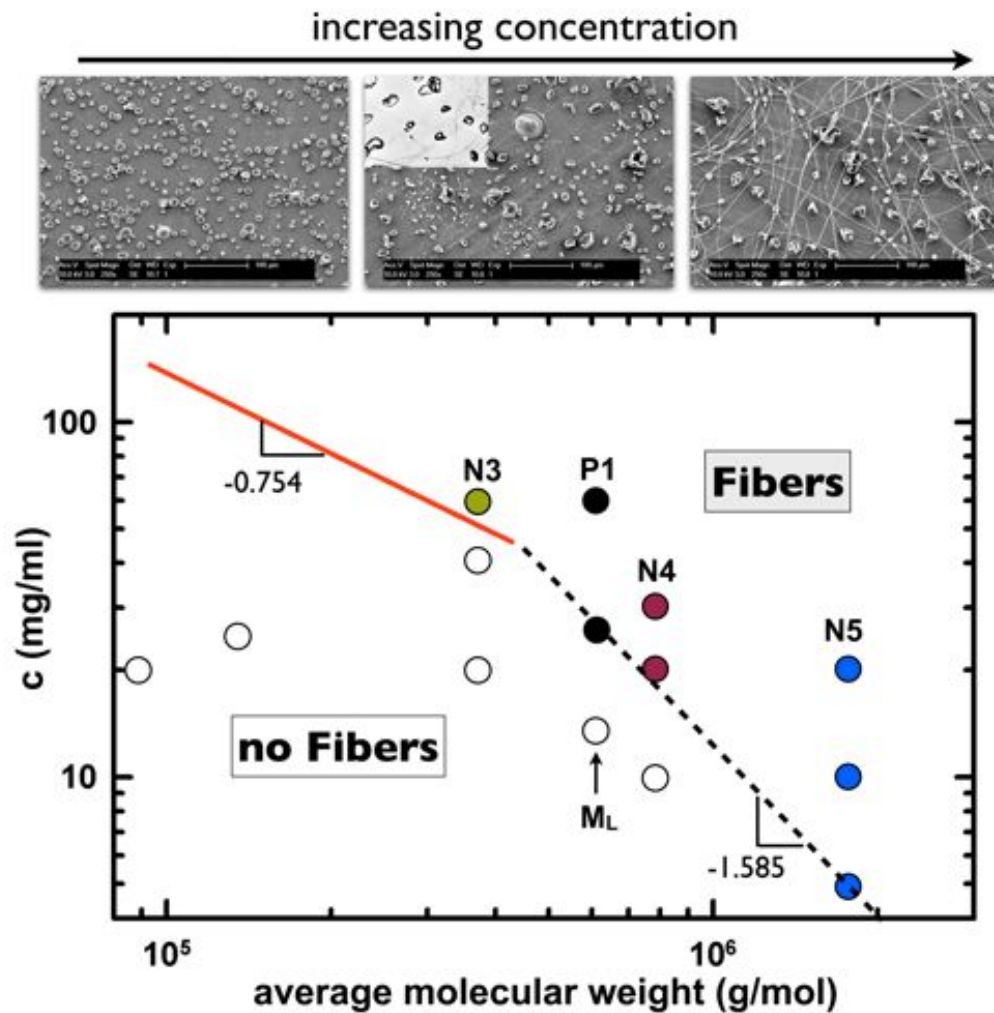
Figure 6: Concentrations of the polydisperse PMMA sample P_1 plotted along with data for the narrowly distributed PMMA samples. While the narrowly distributed sample data is plotted as a function of the weight average molecular weight, for sample P_1 the concentration data is plotted as a function of the extensibility average molecular weight M_L. The solid line represent the critical concentration $10c^*$ (Eq. 1) and the dashed line is the new scaling relation (Eq. 13) for high molecular weights. The SEM images of electrospun products from the polydisperse sample P_1 for the three concentrations are shown above the graph. The inset in the middle image is an enlargement (total image width 100 m) showing the onset of fiber formation at these spinning conditions.
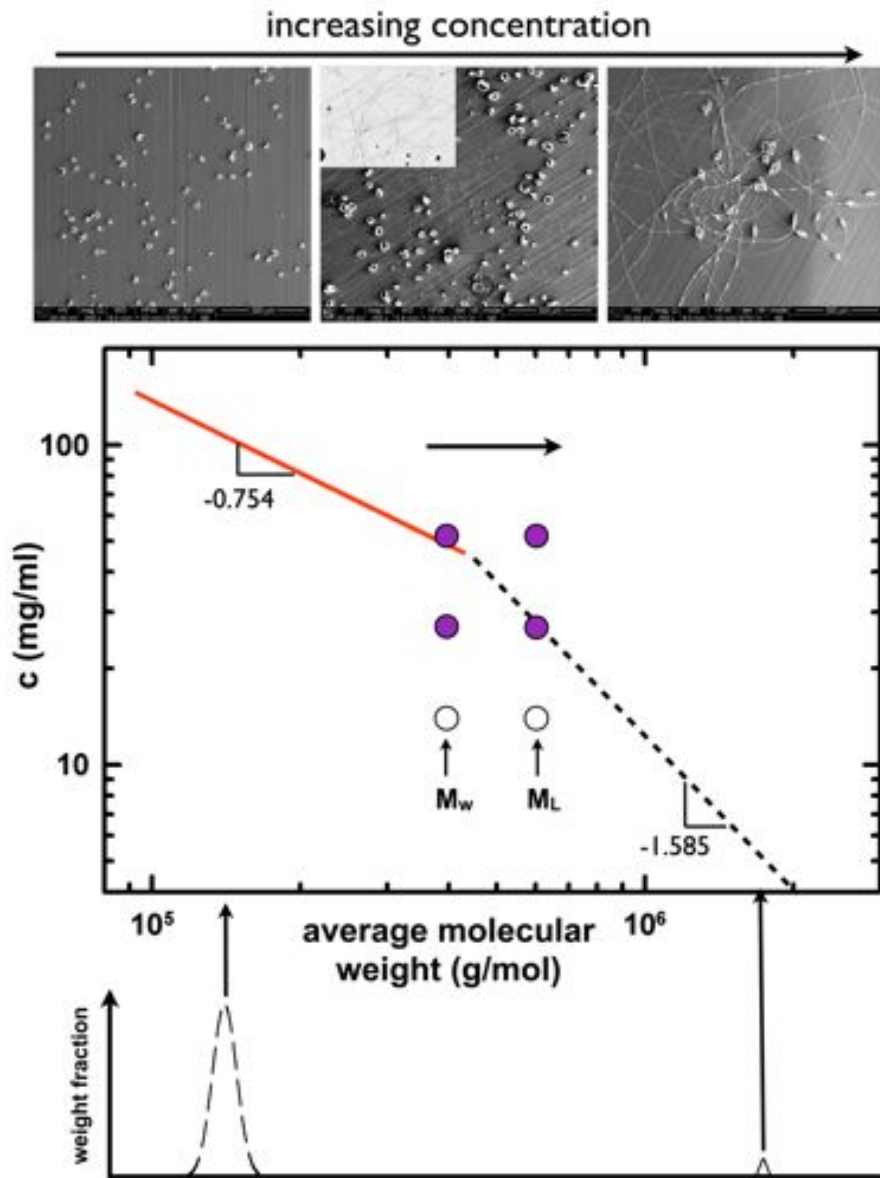
Figure 7: Electrospinning of highly polydisperse PMMA solution formed by a blend of a small amount of a high molecular weight, narrowly distributed PMMA (sample N_5, $w = 0.157$) with a low molecular weight (sample N_2, $w = 0.843$). The molecular weight distribution of the bimodal blend is indicated below the diagram. The morphology of the PMMA samples at three different concentrations after electrospinning is shown above the graph. When plotted in terms of the weight average molecular weight (M_w) of the blend the concentration data does not follow the new scaling prediction (Eq. 13). When plotted as a function of the extensibility average molecular weight (M_L) of the blend the agreement with the extensional stress scaling of Eq. 13 is strongly improved. The insert in the image showing the onset of fiber formation is 250 μm wide.
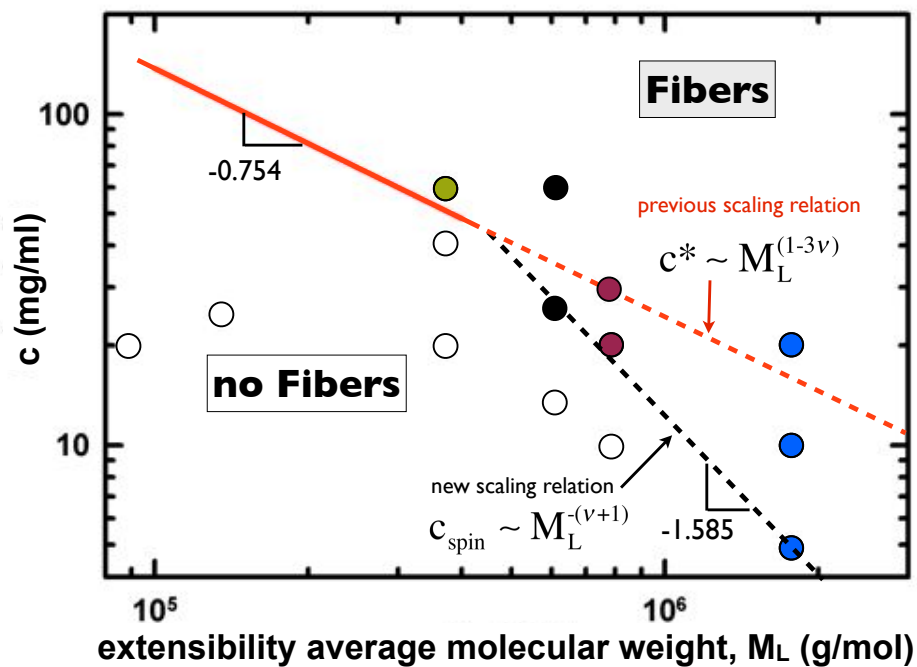
Figure 8: State diagram relating electrospinnability to polymer concentration and the extensibility average molecular weight M_L. A critical concentration for fiber formation can be related to two scaling relations which depend differently on the solvent quality ν: for lower molecular weight the appropriate scaling is based on the overlap concentration c^* which sets the magnitude of the zero-shear viscosity of the spinning solution, and secondly for higher molecular weights the scaling is based on minimum viscoelastic stress and thus a minimum extensional viscosity necessary for fiber formation as indicated in the diagram.